Journal of Applied Polymer Science

Interdiffusion during film formation of ionically cross-linked acrylics investigated with Förster resonance energy transfer (FRET)

Hares Wahdat,[1] Matthias Gerst,[2] Stephan Möbius,[2] Jörg Adams[1]
[1]Institute of Physical Chemistry, Clausthal University of Technology, Clausthal-Zellerfeld D-38678, Germany
[2]Advanced Materials & Systems Research, BASF SE, Ludwigshafen D-67056, Germany
Correspondence to: J. Adams (adams@pc.tu-clausthal.de)

ABSTRACT: Polymer interdiffusion is crucial to obtain continuous films from aqueous polymer dispersions. Here, interdiffusion in films from dispersions of acrylates which were ionically cross-linked prior to film formation was studied by Förster resonance energy transfer analysis. Dispersions of copolymers of n-butyl acrylate, methacrylic acid, and zinc dimethacrylate (ZnDMA) were investigated. ZnDMA was used as a co-monomer to ionically cross link the polymers during the synthesis. Ionic cross-linking does not prevent interdiffusion even at high gel contents. Interdiffusion data were compared with results of tensile tests on final films. Films of ionically cross-linked polymers fracture at both higher stress and strain than films of covalently cross-linked polymers. Further interdiffusion studies addressed effects of temperature and humidity. Both increased temperature and humidity accelerate interdiffusion of ionically cross-linked polymers. Thus, using ZnDMA allows for preparing dispersions which can form continuous films. Also, no volatile organic compounds are released during the film formation. © 2020 The Authors. *Journal of Applied Polymer Science* published by Wiley Periodicals, Inc. J. Appl. Polym. Sci. **2020**, *137*, 48972.

Received 7 August 2019; accepted 4 January 2020
DOI: 10.1002/app.48972

INTRODUCTION

Films from aqueous polymer dispersions are ubiquitously employed as for instance protective coatings, paintings, or adhesives.[1] Polymer dispersions consist of polymer nanoparticles dispersed in water. To prevent aggregation or coalescence in the wet dispersion, the particles are often stabilized by surfactants. Preparing films from dispersions is environmentally friendly in that no or only small amounts of volatile organic compounds (VOCs) are released during drying. However, the film formation process of polymer dispersions is complex and can lead to structural heterogeneities in the final film.[1]

In an idealized view, film formation of polymer dispersions encompasses three subsequent stages, which are drying (stage I), particle deformation (stage II), and polymer interdiffusion (stage III).[1] In stage I, most of the water evaporates and the polymer particles form a sphere packing. Remaining water is located in the interstices, and thus the film still appears turbid. In stage II, the water in the interstices dries out and the particles deform to polyhedra. As a result, the film turns clear. On a nanoscopic scale, the deformed particles are still separated by boundaries. In stage III, the polymer chains from adjacent particles diffuse into each other.[2] Polymer interdiffusion is the crucial step to obtain a mechanically stable, continuous film in which all particles have fused together.[3] Chains from originally different particles form entanglements which provides for cohesive strength in the film. Also, the particle boundaries disappear and a homogeneous film with a continuous entanglement network is formed.[3,4]

In some applications, the cohesion in the polymer film provided by chain entanglements does not suffice for the final application. Often, the cohesive strength is further improved by cross-linking the polymers. However, irreversible, covalent cross-linking of polymer chains reduces their mobility significantly. In case of polymer dispersions, a high degree of irreversible polymer cross-linking prior to film formation can impede the interdiffusion stage during film formation.[5,6] As a result, film formation stops after the particle deformation stage and mechanically weak films are obtained.[5–8] For this reason, formulations used to prepare cross-linked polymer films are designed such that the cross-linking reaction takes place after interdiffusion has finished (post-cross-linking).[9] Post-cross-linking can be achieved by incorporating reactive groups in initially linear chains which do

Additional Supporting Information may be found in the online version of this article.

not cross-link in the wet dispersion but after film formation has finished.[9] Sometimes, VOCs are releases as a by-product of the post-cross-linking reaction.[6] In case of water-borne pressure-sensitive adhesive (PSA) formulations, metal acetylacetonates are added to dispersions of linear polymers to ionically cross-link the polymers in the final film.[6,10–12] Cross-linking takes place after the dispersion starts to dry.[6] As a result of the cross-linking reaction, acetylacetone, a VOC is formed as a by-product.[6,11] Here, we report an alternative route of access to prepare ionically cross-linked polymer films from dispersions which does not involve the release of VOCs.

In the present work, the stage of interdiffusion in films from dispersions of soft acrylics which were reversibly, ionically cross-linked is investigated. Ionic cross-linking occurred prior to film formation and is based on electrostatic interactions between anionic carboxylate groups in the polymer chains and Zn^{2+} ions. Chains can attach and detach from the metal centers in a dynamic equilibrium, and thus the cross-linking is reversible.[13] Since the chains are reversibly cross-linked, interdiffusion should be possible.[6,14] Therefore, in contrast to irreversible, covalent cross-linking, no post-cross-linking step is necessary, and in contrast to ionic cross-linking by metal chelates, no VOCs are released during drying. In general, ionically cross-linked acrylates find use as PSAs.[10–12] The results of the present study can be used to design water-borne PSA formulations. To ionically cross-link the polymers in the dispersion, zinc dimethacrylate [ZnDMA, zinc salt of methacrylic acid (MA)] has been used as a co-monomer during the synthesis. ZnDMA is often used to prepare composites of thermoplastic rubber and poly-ZnDMA.[15] Here, ZnDMA has been employed because it is partially soluble in water. This allows for using it in an emulsion polymerization to synthesize dispersions of ionically cross-linked acrylics.[6] Regarding potential application of such dispersions, often, acrylics cross-linked by Al^{3+} are reported to be used as PSAs.[6,10–12] However, there exist several patents by industry on PSAs based on acrylics cross-linked by Zn^{2+}.[16–18] Again, the ionic cross-links provided by ZnDMA units are governed by electrostatic interactions between anionic carboxylate groups in the MA units and Zn^{2+} cations.[18,19] Previous studies have shown that ionic cross-links between polymeric carboxylate groups and metal cations can be reversible.[13,20–28] Temperature-dependent rheologic analysis of poly(*n*-butyl acrylate)-*co*-poly (acrylic acid) cross-linked by Zn^{2+} ions reported in Ref. 13 has shown that the ionic cross-links between anionic acrylate groups in the polymers and Zn^{2+} are reversible. Therefore, ZnDMA can be used to synthesize aqueous dispersions of reversibly, ionically cross-linked polymers.

The stage of polymer interdiffusion can be tracked by analyzing data from small-angle neutron scattering[29] and Förster resonance energy transfer (FRET)[2] experiments. Recently, interdiffusion has been probed by analyzing excimer formation between pyrene-labeled polymers.[30] In this work, FRET has been used to investigate polymer interdiffusion. In short, FRET is a non-radiative energy transfer process taking place between an excited fluorophore (donor) and a dye in the electronic ground state (acceptor).[31] If the distance between the donor and the acceptor is within 1–10 nanometers, the donor can transfer its excitation energy via dipole-dipole interactions to the acceptor instead of fluorescing. This increases the curvature in the fluorescence decay curve of the donor.[31] Since interdiffusion takes place on nanoscopic scales, FRET analysis can be employed to follow its progress.[2] To study interdiffusion with FRET, a set of two dispersions with identical properties, except for the labeling must be prepared. In one dispersion, fluorescent donor-dyes are covalently attached to the polymers, and in the other one, acceptor-dyes are attached to the polymers. A blend of labeled dispersions is cast and interdiffusion is tracked by continuously recording donor fluorescence decays in a kinetic experiment. While the labeled polymers intermix due to interdiffusion, the curvature in the donor decays increase. Analysis of the change of the curvature allows for quantifying the progress of polymer interdiffusion.[2]

Since the early 1990s, most of the interdiffusion studies were carried out based on FRET analysis.[2] Compared with neutron scattering, probing interdiffusion by FRET is experimentally less demanding. Also, to study interdiffusion, the FRET analysis is usually carried out on data obtained from time-resolved fluorescence measurements. Time-resolved fluorescence is suitable to easily obtain quantitative data from samples which change their optical properties during the experiment such as drying polymer dispersions. A brief literature review on previous findings relevant to the present work is presented in the following. The first interdiffusion studies based on FRET analysis targeted coatings,[2,32] and thus, most of the fundamental results were obtained on those materials. Increasing temperature promotes interdiffusion.[2] Usually, the polymers in dispersions have a broad molecular weight distribution. In films from polymer dispersions, interdiffusion is initially dominated by chains with low molecular weight due to their higher mobility compared with the chains with high molecular weight which diffuse much slower.[2] Irreversible, covalent cross-linking prevents interdiffusion.[5,33] Also, interdiffusion of polymers which can undergo a cross-linking reaction after drying starts has been investigated (post-cross-linking).[9,34–37] By combining FRET studies with theoretical models, it was concluded that interdiffusion must be faster than the cross-linking reaction to obtain a continuous film.[9,38,39] In the present study, the effects of humidity on interdiffusion was addressed as well for reasons given in the next paragraph. It has been shown by differential scanning calorimetry (DSC) measurements that polymer films made from dispersions have a reduced glass transition temperature, T_g, when water is dissolved in their matrix (hydroplasticization).[40] FRET studies have shown that hydroplasticization accelerates polymer interdiffusion.[33,41,42] Recent studies addressed polymer interdiffusion in film forming water-borne PSA dispersions.[6,33] Because of the low T_g of the polymers, interdiffusion at room temperature is fast to the extent that is almost finished immediately after the polymer particles deform and come into contact.[33] Furthermore, blends of industrially relevant dispersions of linear polymers blended with the ionic cross-linker aluminum acetylacetonate have been studied.[6] The cross-linking reaction by aluminum acetylacetonate mainly takes place after film formation starts. FRET studies suggest that the cross-linking reaction is slower than interdiffusion.[6] Also, within a comparative study in Ref. 6, interdiffusion in a film of polymers ionically cross-linked by ZnDMA was examined. It was found that ionic cross-linking slows down interdiffusion. Still, after homogenization of the film with tetrahydrofuran (THF) followed

by annealing, a significant increase of the interdiffusion parameter has been observed, which indicates that ionic polymer cross-linking by ZnDMA does not hinder interdiffusion.[6] In the present work, the result from Ref. 6 is evaluated by performing a systematic study on model dispersions.

In this work, interdiffusion in films from aqueous dispersions of copolymers *n*-butyl acrylate (BA), MA, and ZnDMA was investigated by FRET analysis. The main repetition unit in the copolymers is BA, and thus the final copolymers have a T_g well below 0 °C. The degree of ionic cross-linking was adjusted by varying the ratios of MAA and ZnDMA during the synthesis. Interdiffusion in films from dispersions of ionically and covalently cross-linked polymers, which both have similar gel contents, was compared with each other. The cohesive strength in final films was evaluated by tensile tests. Results of tensile tests on films from dispersions can often be correlated with the stage of polymer interdiffusion.[4–7,43] As chains interdiffuse, a continuous entanglement network is formed throughout the film which leads to an increase of both the peak stress and the strain at failure.[43] Further studies in the present paper concern the effects of temperature and relative humidity, rH, on interdiffusion. Again, increasing temperature accelerates interdiffusion.[2] Also, the ionic bond between carboxylate groups in the polymers and Zn^{2+} is thermally reversible.[13] At increased temperatures, the polymers can detach from the metal centers more easily, which is expected to promote interdiffusion.[13] The influence of rH was studied because Zn^{2+} ions in films made from dispersions are known to absorb water vapor,[44] which can lead to hydroplasticization.

EXPERIMENTAL SECTION

Chemicals

If not mentioned otherwise, all chemicals have a purity of at least 99% and were purchased from Sigma Aldrich. BA and MA were purified using inhibitor remover resins. Water was de-ionized using an Arium661 VF system (Sartorius). ZnDMA, methyl ethyl ketone (MEK), (9-phenanthryl)methyl methacrylate (Phen-MMA, Toronto Research Chemicals), 1-(4-nitrophenyl)-2-pyrrolidonemethyl acrylate (NPP-A, 97%), THF (spectroscopic grade, Alfa Aesar), acetylacetone (Alfa Aesar), sodium dodecyl sulfate (SDS, Carl Roth), *n*-dodecyl mercaptan (DDM), hexadecane (HD, Merck Millipore), sodium persulfate (NaPS, Merck), ethylene glycol dimethacrylate (EGDMA, 98%), silica gel, sodium bromide (NaBr), and sodium chloride (NaCl) were used as received.

Characterization of Polymer Dispersions

Solids contents were determined gravimetrically. Hydrodynamic diameters were measured by dynamic light scattering (ALV/CGS-3, 633 nm, detection angle: 90°, temperature: 25 °C). The hydrodynamic diameter, d_h, and the polydispersity are provided. Molecular weight distributions of the polymers were determined by gel permeation chromatography (GPC, Agilent 1200, SDV/PSS columns) on samples dried films from dispersions. The eluent was freshly distilled THF, the standard used for calibration was polystyrene and the temperature was 25 °C. The weight average of the molecular weight, M_w, and the polydispersity are provided. Glass transition temperatures, T_g, of polymers were determined by DSC (Mettler Toledo, heating curves: −80 to +100 °C, rate: 10 °C/min). Polymers dried from dispersions were measured. The dispersions were first dried for four days at room temperature and then at vacuum overnight. Gel contents were determined as follows: Rectangular polymer pieces with a final thickness of ~1 mm were dried from dispersions. The dispersions were first dried for four days at room temperature and then overnight at 40 °C. The polymer pieces were swollen in MEK. The mass of the MEK was 100 times the mass of the polymer piece. After swelling for three days, the gel was separated by filtration using 120 µm nylon filters (Sefar Nitex). The gel content was calculated as $100\%\cdot(m_{gel}/m_{polymer})$, with $m_{polymer}$ being the mass of the polymer piece before swelling and m_{gel} being the mass of the dry gel collected by the filter.

Synthesis of Polymer Dispersions

Acrylic polymer dispersions were prepared by miniemulsion polymerization initiated in the *aqueous* phase. The process of miniemulsion polymerization is described in Ref. 45. Here, miniemulsion polymerization was employed because it allows for the preparation of small volumes (~10 mL) of stable dispersions, and thus only small amounts of the expensive monomeric FRET-dyes need to be used. For FRET studies, sets of two dispersions with identical properties, except for the labeling, were prepared. Monomeric dye-labels were Phen-MMA (donor, "D") and NPP-A (non-fluorescent acceptor, "A").[46] They were added at constant amounts. Preparing dispersions with different degrees of ionic polymer cross-linking was achieved by varying the composition of the monomer phase consisting of BA, MAA, and ZnDMA, as shown in Table I. "L" denotes that chains are linear and "Zn-X" denotes that chains are ionically cross-linked by Zn^{2+}. In case of "Zn-X-1," the molar ratio of COOH to Zn^{2+} was 2/1 (stoichiometric cross-linking), and in case of "Zn-X-0.5" it was 4/1 (half-stoichiometric cross-linking). In all dispersions, the weight ratio of m_{BA}/m_{COOH} was 98/2. Please note, that "COOH" denotes either the acid form or the anionic carboxylate form, with MAA providing for one carboxylate group and ZnDMA providing for two carboxylate groups. For comparative studies, dispersions of irreversibly, covalently cross-linked polymers were synthesized (D-cov-X and A-cov-X) by using EGDMA as a co-monomer during the synthesis. The monomer composition was $m_{BA}/m_{EGDMA}/m_{MAA}$ = 94/4/2 (see Table II). Composition of phases during miniemulsion polymerization and masses of components added

Table I. Masses of Monomers Used During the Synthesis of Dispersions with Varying Degree of Ionic Cross-linking

Dispersion	m_{BA} (g)	m_{MAA} (g)	m_{ZnDMA} (g)	m_{dye} (g)
D-L	1.787	0.035	0	0.029
A-L	1.797	0.036	0	0.018
D-Zn-X-0.5	1.778	0.018	0.029	0.029
A-Zn-X-0.5	1.787	0.018	0.029	0.018
D-Zn-X-1	1.765	0	0.058	0.029
A-Zn-X-1	1.775	0	0.058	0.018

Dyes were Phen-MMA and NPP-A in case of donor (D)- and acceptor (A)-labeling, respectively.

Table II. Masses of Monomers Used During the Synthesis of Dispersions with Covalently Cross-linked Chains

Dispersion	m_{BA} (g)	m_{MAA} (g)	m_{EGDMA} (g)	m_{dye} (g)
D-cov-X	1.712	0.036	0.073	0.029
A-cov-X	1.722	0.036	0.073	0.018

Dyes were Phen-MMA and NPP-A in case of donor (D)- and acceptor (A)-labeling, respectively.

Table III. Composition of Phases and Masses of Reagents Added at Constant Amounts

Phase	Chemicals
Aqueous phase	Water (6 g), SDS (0.037 g, 2 pphm), ZnDMA (varied)
Organic phase	Monomers (varied), HD (0.074 g, 4 pphm), DDM (0.002 g, 0.1 pphm)
Initiator solution	Water (2 g), NaPS (0.037 g, 2 pphm)

Masses of monomers are provided in Tables I and II. pphm: parts per hundred monomers.

at a constant amount are given in Table III. "pphm" stands for parts per hundred monomer and is the weight percentage with respect to the total mass of the monomers. Note, that ZnDMA was dissolved in the *aqueous phase* because it is not soluble in the monomer phase.

Miniemulsion polymerization was carried out as follows: The aqueous and organic phases were prepared in separate vials. Then, both phases were intermixed in one single vial. The vial was placed in an ice bath and the mixture was sonicated for 2 min (duty cycle 70%, output 7, Branson Sonifier). Afterwards, the initiator solution was added. The vial containing the mixture was purged with argon for five minutes and then sealed. The vial was placed in a thermo-shaker (HTA Biotech) and the polymerization was started. The polymerization reaction was carried out by keeping the mixture at a temperature of 60 °C for 8 h.

Properties of Polymer Dispersions

Properties of donor- ("D") and acceptor-labeled ("A") polymer dispersions are provided in Table IV (linear chains) and Table V (cross-linked chains). T_g data are not provided for these polymers since they could not be determined by DSC because HD in the films smeared out the inflection points. To evaluate whether cross-linking by ZnDMA increases the polymer's T_g unlabeled dispersions were prepared by batch emulsion polymerization without the addition of HD. T_g values of polymers in films from dispersions with linear chains and ionically cross-linked chains by ZnDMA (stoichiometric cross-linking, 75% gel content) were measured to be −50 °C, implying that cross-linking by Zn^{2+} does not increase the T_g. This finding is consistent with the results of the authors of Ref. 13. They also did not observe an increase of T_g when cross-linking poly(*n*-butyl acrylate)-*co*-poly(acrylic acid) copolymers by Zn^{2+}.[13] Please see the Supporting Information, Section 2, Figure S2 for the corresponding DSC curves of the polymers in the herein investigated dispersions.

Table IV. Properties of Dispersions with Linear Chains

Dispersion	Solids content (%)	d_h (nm)	M_w (kg/mol)
D-L	19.0	151 (1.1)	504 (2.9)
A-L	19.1	134 (1.0)	298 (2.1)

The number in parentheses is the polydispersity.

Table V. Properties of Dispersions with Cross-linked Chains

Dispersion	Solids content (%)	d_h (nm)	Gel content (%)
D-Zn-X-1	17.0	212 (1.1)	80
A-Zn-X-1	19.1	246 (1.2)	79
D-Zn-X-0.5	17.5	182 (1.0)	38
A-Zn-X-0.5	18.6	180 (1.1)	40
D-cov-X	19.2	127 (1.0)	71
A-cov-X	19.8	149 (1.1)	79

Zn-X-1: stoichiometric cross-linking, Zn-X-0.5: half-stoichiometric cross-linking. The number in parentheses is the polydispersity.

As shown in Table IV, donor- and acceptor-labeled dispersions have similar properties. GPC measurements for D-L and A-L, where UV sensors sensitive to the respective label were applied, reveal that the dyes are distributed along all chains (GPC data are provided in the Supporting Information, Section 1, Figure S1).

In Table V, properties of dispersions with ionically ("Zn-X") and covalently ("cov-X") cross-linked chains are provided. The properties are comparable within a set of labeled dispersions. Gel contents increase with increasing amount of cross-linker. With increasing amount of ZnDMA, the particle size increases. It is assumed that the increase of particle size is associated with a decreased colloidal stability in the dispersions. The decreased colloidal stability results from employing a reduced amount of MAA during the synthesis of dispersions cross-linked by ZnDMA. Generally, in polymer dispersions prepared by emulsion polymerization, MAA is known to be mostly incorporated in the polymer chains within the particles.[47,48] However, a small fraction of water-soluble oligomers containing MAA is formed as well.[48] Due to their water-solubility, these oligomers can be located in the surfactant shell between the polymer phase in the interior of the particles and the water phase. Such oligomers are known to act as co-surfactants which further stabilize the particles against aggregation.[49] Here, the dispersions were synthesized by miniemulsion polymerization initiated in the aqueous phase, and therefore it can be expected that water-soluble oligomers containing MAA are formed. Also, in all of the herein studied dispersions, the number of carboxylate groups is equal. Carboxylate groups are provided by either MAA or ZnDMA. As with increasing amount of ZnDMA, the amount of MAA decreases, less co-surfactants are expected to be formed during the synthesis. This is assumed to lead to a decreased colloidal stability, and thus a larger particle size in the final dispersion.

Study of Interdiffusion by FRET Analysis

The investigation of polymer interdiffusion in film forming dispersion was based on FRET studies quantified by time-resolved fluorescence. Fluorescence decays of the donor were recorded by time-correlated single-photon counting. A custom-built instrument was employed. Details about the instrument as well as the sample preparation and measurement are provided in Ref. 33. FRET studies were carried out on 1/1 (*m*/*m*) blends of donor- and acceptor-labeled dispersions ("DA") with otherwise identical properties. Blends of labeled dispersions were prepared by intermixing them for ~30 s followed by casting on microscope slides. The microscope slides were then immediately placed into the measurement chamber and the measurement was started. Casting volume was 3 μL, spot size of the film was ~16 mm,[2] wet film thickness was ~190 μm and the dry film thickness was ~40 μm. The maximum observation depth for the experiment was calculated to be ~5.5 μm (see Ref. 33 for the calculation). In all cases, the center of the film was studied. The width of focal spot of the pulsed light emitting diode was 1 mm. The temperature was always 21 °C and the relative humidity, rH, was varied depending on the experiment (see the following paragraph).

FRET was quantified by recording donor fluorescence decays and analyzing their curvature. To follow the progress of interdiffusion in a film forming dispersion, donor decays were continuously recorded in a kinetic experiment. Accumulation time usually was 30 s. The number of counts at the decay's maximum was always at least 2×10^4. If not mentioned otherwise, films were dried with a stream of dry air (leading to 3% rH) which was turned on after the first decay in a kinetic experiment has been recorded. To study the effect of rH on interdiffusion, humidity control agents were placed into the measurement chamber prior to the experiment. Silica gel (10% rH), aqueous, saturated solutions of NaBr (56% rH) and NaCl (75% rH) or pure water (92% rH) were employed. For thermal annealing experiments, the films were first dried at room temperature until becoming transparent. Afterwards, they were placed in an oven at a fixed temperature for a certain time. After a given annealing time, the films were removed from the oven, allowed to cool down to room temperature and the donor decay was measured.

Donor fluorescence decays were fitted to the respective model by minimizing the weighted residues, χ^2, using the Levenberg-Marquardt algorithm. In all cases, the lamp shift and the background noise entered the fit function. χ^2 was never larger than 2 (at least $2 \cdot 10^4$ counts at the decay's maximum). To quantify the progress of polymer interdiffusion, the donor fluorescence decays were fitted according to the two-state model [eq. (1)] which has been developed by the Winnik group.[2] Central aspects of the two-state model are briefly introduced here. A more detailed description is provided in Ref. 2.

$$I(t') = I_0 \left[A_2 \cdot \exp\left(\left(-\frac{t'}{\tau_D} \right) - 2\gamma \sqrt{\frac{t'}{\tau_D}} \right) + (1 - A_2) \cdot \exp\left(-\frac{t'}{\tau_D} \right) \right] \quad (1)$$

$$f_m(t) = \frac{A_2(t) - A_{2,\min}}{1 - A_{2,\min}} \quad (2)$$

In eq. (1), t' is the decay time in nanoseconds and I_0 is the intensity immediately after the excitation pulse. A_2 is the central fit parameter. It increases as interdiffusion progresses. In general, the value of A_2 is related to the fraction of donors which have intermixed with acceptors and are capable of performing FRET as a result. τ_D and 2γ are kept constant during fitting after being determined in separate experiments. τ_D is the fluorescence lifetime of the donor. It was obtained from a dried film consisting of donor-labeled chains only ($A_2 \equiv 0$, mono-exponential decay) and was determined to be 40.0 ns. 2γ is related to the FRET efficiency in a film in which donors and acceptors have fully intermixed ($A_2 \equiv 1$, maximum curved decay which is described by the Förster equation). This state is achieved by intermixing dry films consisting of linear chains with THF and annealing them afterwards at 60 °C overnight (in the following, these films are termed "THF film"). 2γ was determined to be 1.63.

A_2 was converted to the fraction of intermixing, f_m, following eq. (2).[2] For the data analysis, f_m is plotted against the film formation time t, the latter in units of seconds or minutes. The time defined as $t \equiv 0$ is discussed in the following and in the Supporting Information, Section 2.

In eq. (2), $A_{2,\min}$ is the A_2 value obtained from a fit of a fluorescence decay of a wet, non-drying blend of donor- and acceptor-labeled dispersions.[33] Drying of the dispersions was prevented by sealing them in UV-transparent quartz cells during the measurement. The value of $A_{2,\min}$ is related to the state of intermixing of labeled chains in the dispersion prior to drying. $A_{2,\min}$ was found to be ~0.2 for all dispersion systems. Intuitively, a value close to zero is expected because no interdiffusion has taken place. The reason for a value above zero is associated with the formation of labeled, water-soluble oligomers which exchange between the particles after donor- and acceptor-labeled dispersions are intermixed.[33,42] Water-soluble oligomers are a known by-product in emulsion polymerization.[50,51] Here, the dispersions were prepared by miniemulsion polymerization initiated in the *aqueous* phase, similar to emulsion polymerization, and thus the formation of water-soluble oligomers can be expected. For labeled dispersions prepared by conventional miniemulsion polymerization, which is initiated inside the polymer particles by an oil-soluble initiator, the formation of water-soluble oligomers is negligible and $A_{2,\min}$ was found to be around 0.1.[52]

In all experiments, in addition to emitted fluorescent light, the intensity of scattered excitation light was detected simultaneously. Semi-log plots of f_m and I_{scat}, which is a background-subtracted and normalized scattering intensity,[33] against time for a film forming dispersion are shown in Figure 1. f_m is associated with the progress of polymer interdiffusion and I_{scat} with the progress of drying and particle deformation. Please note, that in eq. (2), $t = 0$ is *not* the time immediately after casting the dispersion and starting the measurement. Rather, the time chosen to be $t = 0$ in eq. (2) (to plot the curves in Figure 3) is marked by the *solid blue line* in Figure 1. At this time the intensity of scattered excitation starts to sharply decrease to zero. Simultaneously, f_m strongly increases. The processes before the solid blue line are discussed in Ref. 33. In principal, they are a consequence of heterogeneous top-down drying combined with an increase of the observation

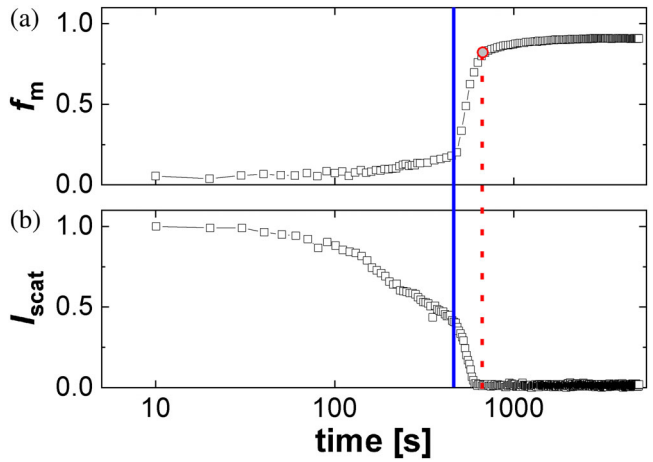

Figure 1. Complete FRET (indicative for interdiffusion) (a) and light scattering (indicative for particle deformation) data (b) for a film forming dispersion. The solid line marks the time chosen to be $t = 0$ in eq. (2). For plots in Figure 7, one representative f_m value has been used to describe the interdiffusion kinetics of the sample. The f_m data point when I_{scat} reaches zero has been chosen. In the plot above, this is indicated by the circle connected to the dotted line. [Color figure can be viewed at wileyonlinelibrary.com]

Table VI. Properties of Dispersions Used for Tensile Tests

Dispersion	d_h (nm)	M_w (kg/mol)	Gel content (%)
L	218 (1.2)	291 (3.4)	0
Zn-X	251 (1.1)	-	82
cov-X	216 (1.1)	-	89

Solids content is 52% in all cases. The number in parentheses is the polydispersity.

depth during the experiment. For all dispersions dried under identical conditions, the sharp decrease of I_{scat} to zero occurs at around the same time, indicating that drying and deformation kinetics are unaffected by the polymer architecture (see the Supporting Information, Section 3, Figure S4 for full film formation kinetics of all dispersions). Once I_{scat} has become zero, it can be expected that no significant drying takes place. Also, the maximum observation depth for the experiment is reached as no excitation light is scattered anymore. In Ref. 33, the observation depth was calculated to be 5.5 μm. There is a strong increase of f_m taking place simultaneously with the sharp decrease of I_{scat} (Figure 1). The strong increase of f_m occurs because particles come into contact and interdiffusion starts.[33] The magnitude of the increase of f_m is affected by cross-linking as will be shown in Section 3.1. To study the influence of ambient humidity on interdiffusion, f_m data of film forming dispersions with identical polymer architecture dried at variable rH were compared with each other (Figure 7). Single f_m data points at the time when I_{scat} becomes zero were plotted against rH. The f_m data point and the corresponding time are marked by the *circle* and *dotted* line in Figure 1, respectively. After I_{scat} has become zero for all samples that were compared with each other, there are no intersection points between the f_m-curves. Thus, one data point can be chosen to be representative for the entire interdiffusion kinetics. The complete f_m and I_{scat} data are provided in the Supporting Information, Section 3, Figure S5.

To estimate polymer diffusion coefficients, D, selected f_m data covering the entire film formation time were fitted to the spherical diffusion model [eq. (3)][53] following eq. (4), as suggested by Winnik.[2] Please find details and simplifications made by using this fitting procedure in Refs. 54 and 55.

$$C(r,t) = \frac{C_0}{2}\left[\mathrm{erf}\left(\frac{R+r}{2\sqrt{Dt}}\right) + \mathrm{erf}\left(\frac{R-r}{2\sqrt{Dt}}\right)\right] - \frac{C_0}{R}\sqrt{\frac{Dt}{\pi}} \times \left\{\exp\left[-\frac{(R+r)^2}{4Dt}\right] - \exp\left[-\frac{(R-r)^2}{4Dt}\right]\right\} \quad (3)$$

$$f_m(t) \approx 1 - \frac{3}{4\pi R^3 C_0}\int_0^R C(r,t)4\pi r^2 dr. \quad (4)$$

The value of D obtained from eq. (4) can be interpreted to be an apparent, cumulative diffusion coefficient of all chains having intermixed as a result of interdiffusion at a given time t.[2] In eq. (3), C_0 is the initial concentration, R is the average radius of labeled particles, which is calculated as $R = d_h/2$, and r is the diffusion distance in nanometers.

Tensile Tests

To evaluate the mechanical strength, tensile tests were performed on polymers dried from industrially relevant dispersions (see Table VI for properties). The polymers in the dispersions have the same architecture as the ones in the dispersions that were used for interdiffusion studies (discussion is provided in the next paragraph). A Zwick 1465 instrument (ISO 527-2, DIN 53504 S3A) was used for the tensile tests. Specimens were polymer strips having widths of 4 mm, lengths of 30 mm, and thicknesses between 0.8 and 1.2 mm. The samples were prepared by drying the respective dispersion for 10 days at 23 °C and 50% rH. Testing speed was always 1000 mm/min. For each system, at least five samples were measured. Representative plots of the engineering stress, σ, versus the engineering strain, ε, are shown in this manuscript. In addition, the peak stress, σ_{max}, the strain at fracture, ε_{frac}, and the elastic modulus in the linear regime within the low-strain limit, E, are provided.

For the tensile tests, unlabeled dispersions with higher solids content were prepared (52%). A higher solids content increases the viscosity in the dispersion. From these viscous dispersions, samples with a uniform thickness could be dried. Also, the dispersions have industrial relevance and were prepared by semi-batch emulsion polymerization. Their synthesis and exact composition are described in Refs. 6 and 34. The properties of the dispersions are summarized in Table VI. Dispersions of linear ("L"), ionically cross-linked ("Zn-X," stoichiometric cross-linking) and covalently cross-linked ("cov-X") polymers were prepared. With respect to the polymer architecture, the interdiffusion kinetics of these dispersions are expected to be similar to the interdiffusion kinetics of the herein studied model dispersions.[6] Also, for the films dried from the dispersions in Table VI, no increase of T_g as a result of

cross-linking by ZnDMA was observed. In all cases, a T_g of −30 °C was measured by DSC. The corresponding DSC curves are provided in the Supporting Information, Section 2, Figure S2.

RESULTS AND DISCUSSION

Influence of Reversible, Ionic Cross-Linking on Interdiffusion

Interdiffusion kinetics of the dispersions DA-L (linear), DA-Zn-X-0.5 (half-stoichiometric cross-linking by Zn^{2+}), DA-Zn-X-1 (stoichiometric cross-linking by Zn^{2+}), and DA-cov-X (covalent cross-linking) are shown in Figure 2. In all cases, polymer cross-linking occurred prior to film formation. The evolution of the fraction of intermixing, f_m [eq. (2)], over the film formation time t is associated with the progress of polymer interdiffusion. Shortly after the first data point, there is a strong increase of f_m at ~100 s in all data sets except for DA-cov-X. The initial increase of f_m occurs because the deformed polymer particles come into contact and chains immediately start to interdiffuse. Following the strong increase of f_m which persists up to around 400 s, the f_m-curves flatten but still continuously increase due to polymer interdiffusion in all films. Interdiffusion is fastest for DA-L. With increasing degree of polymer cross-linking, interdiffusion becomes slower. The interdiffusion kinetics between DA-Zn-X-1 and DA-cov-X are similar. In both cases, the polymers have a similar gel content of around 80% (see Table V). Also, the polymers were cross-linked *prior to* film formation. However, while at room temperature, the interdiffusion kinetics between DA-Zn-X-1 and DA-cov-X-1 are comparable, they differ at elevated temperatures. Thermal annealing further increases f_m in case of DA-Zn-X-1, whereas almost no increase of f_m has been observed in case of DA-cov-X. Results of thermal annealing experiments for DA-Zn-X-1 are shown in Figure 3. The increase of f_m is proportional to the annealing temperature. For DA-Zn-X-0.5, this increase is more pronounced (data not shown here) due to the lower degree of cross-linking. Again, no significant increase of f_m was observed when annealing DA-cov-X because the chains are irreversibly cross-linked, which prevents interdiffusion.[5,6] The increase of f_m when thermally annealing films of ionically cross-linked polymers (DA-Zn-X-0.5 and DA-Zn-X-1) can be explained by the reversibility of the bond between carboxylate groups in the polymers and Zn^{2+} ions.[13] Chains can reversibly detach from the metal centers and interdiffuse.[13] The final states of intermixing, meaning the maximum extent of interdiffusion possible in each film, were achieved by homogenization of the respective film with THF followed by annealing at 60 °C. The maximum values of f_m are 1 (DA-L), 0.98 (DA-Zn-X-0.5), 0.87 (DA-Zn-X-1), and 0.38 (DA-cov-X) ("THF film" in Figure 2).

For a more quantitative analysis of the interdiffusion kinetics, selected f_m data from Figure 2 covering the entire time were fitted according to the spherical diffusion model [eq. (4)]. This allows for the estimation of cumulative diffusion coefficients D. In all films, D decreases with increasing f_m, starting from 1 to 10 nm^2/s and eventually descending to 0.1–1 nm^2/s (Figure 4). This is attributed to the broad molecular weight distribution of the

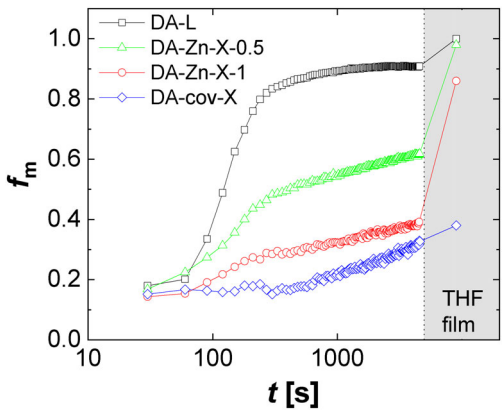

Figure 2. Progress of interdiffusion for DA-L, DA-Zn-X-0.5, DA-Zn-X-1, and DA-cov-X. f_m values after the dotted line indicate the maximum degree of intermixing possible, which was achieved by homogenization with THF (THF film). Please note that the first data point is not the one recorded immediately after casting the film and starting the measurement. Processes occurring before the first data points at t = 30 s are unaffected by the polymer architecture (see Figure 1 and the Supporting Information, Section 3, Figure S3). Rather, they are a consequence of the softness of the polymer particles. A detailed explanation is provided in Ref. 33. [Color figure can be viewed at wileyonlinelibrary.com]

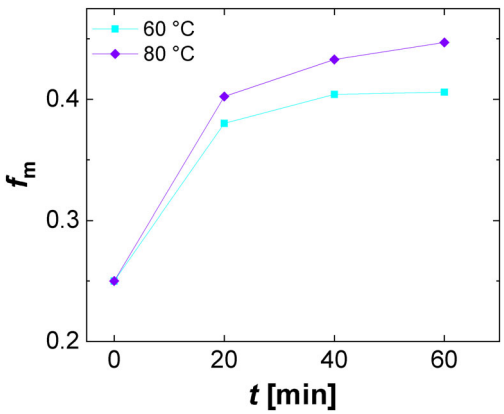

Figure 3. Influence of temperature on interdiffusion for DA-Zn-X-1. The film was annealed for a certain time at a fixed temperature. The FRET measurement was carried out after the film has cooled down to room temperature. [Color figure can be viewed at wileyonlinelibrary.com]

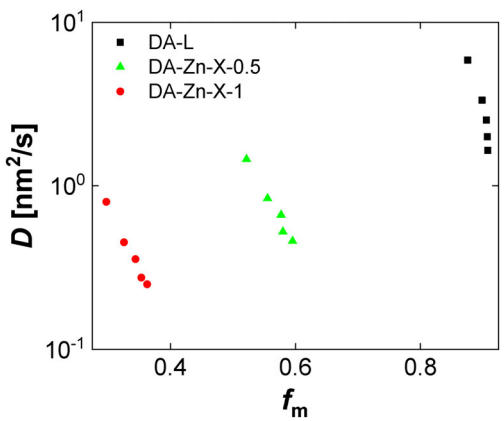

Figure 4. D versus f_m. Data for t ~500, 1000, 1500, 2000, and 2500 s are shown. [Color figure can be viewed at wileyonlinelibrary.com]

polymers.[30,55] At short times, interdiffusion is dominated by the small, fast chains while at later times, only the large, slow chains can contribute to the further increase of f_m.[55] With increasing degree of cross-linking, the curves are shifted to lower f_m values because the ionic cross-links, despite being reversible, retard interdiffusion. At high degrees of cross-linking (DA-Zn-X-1), thermal annealing is necessary to achieve the state of complete interdiffusion.

In an intermediate summary, it can be stated that ZnDMA allows for the preparation dispersions of ionically cross-linked acrylics which form continuous films after casting. Despite the cross-links, the stage of interdiffusion during film formation is still possible. Thus, mechanically stable films can be made from the dispersions (see Section 3.2 for results of tensile tests). Furthermore, no VOC is released during the film formation process. The results of the herein presented study can for instance be helpful to design water-borne formulations of acrylic PSAs.

Tensile Tests

Tensile tests were performed on polymer samples made from unlabeled dispersions (see Table VI for properties). The film with linear chains (L) does not fracture and flows until the end of the experiment (up to ε = 3000%) whereas the films with ionically (Zn-X) and covalently cross-linked chains (cov-X) fracture due to higher cohesion provided by the cross-links (Figure 5). The elastic moduli in the low-strain regime, E, seem to be rather unaffected by cross-linking; the differences mainly concern the strain at failure, ε_{frac}, and the peak stress, σ_{max} (Figure 6). Compared with cov-X, Zn-X has much higher values of ε_{frac} and σ_{max}. The improved cohesive properties of Zn-X are assumed to be the consequence of a more pronounced polymer interdiffusion during film formation. Ionic cross-linking allows for interdiffusion, and thus a film with a continuous network of cross-links and polymer entanglements is formed. The entanglement network provides for additional cohesive strength,[5,6,9] which increases ε_{frac} and σ_{max} for Zn-X.

Influence of Relative Humidity

The influence of relative humidity, rH, on interdiffusion was studied for DA-L, DA-Zn-X-0.5 and DA-Zn-X-1. In Figure 7, single data points of f_m which were found to be representative for the entire interdiffusion kinetics of the respective sample are plotted against rH. Please see the Supporting Information, Section 2, Figure S5 for full film formation kinetics and a detailed explanation regarding the data analysis.

Increasing rH from 10 to 75% accelerates interdiffusion in all films (Figure 7). This acceleration can be attributed to hydroplasticization, which has been observed for films from water-borne coatings[41,42] and PSA[33] formulations as well. The main repetition unit in the polymers investigated in Figure 7 is BA. Hydroplasticization in poly(*n*-butyl acrylate) films dried from dispersions has been shown by DSC measurements in Ref. 40.

However, further increase of rH from 75 to 92% leads to a decrease of f_m in case of DA-L and DA-Zn-X-0.5, and an increase of f_m in case of DA-Zn-X-1. Also, all films dried at 92% rH were turbid, whereas they were transparent at lower rH. First, an

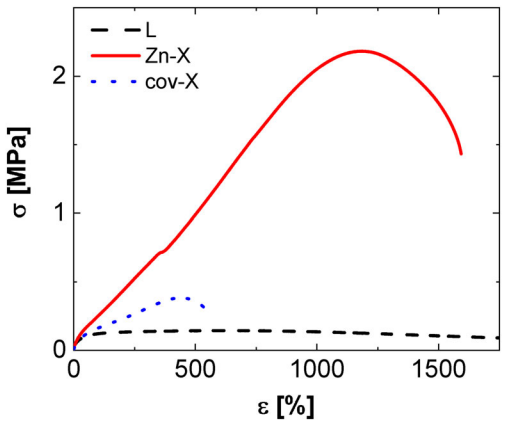

Figure 5. Stress-strain curves from tensile tests for L, Zn-X, and cov-X. [Color figure can be viewed at wileyonlinelibrary.com]

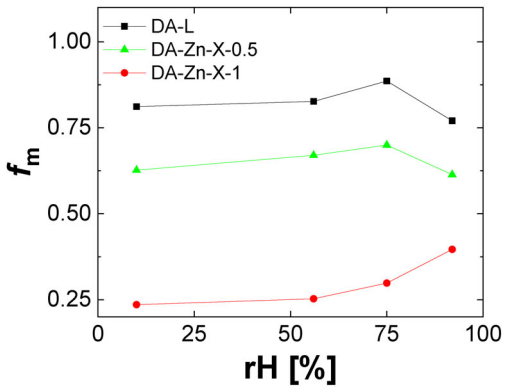

Figure 7. Influence of relative humidity on interdiffusion. [Color figure can be viewed at wileyonlinelibrary.com]

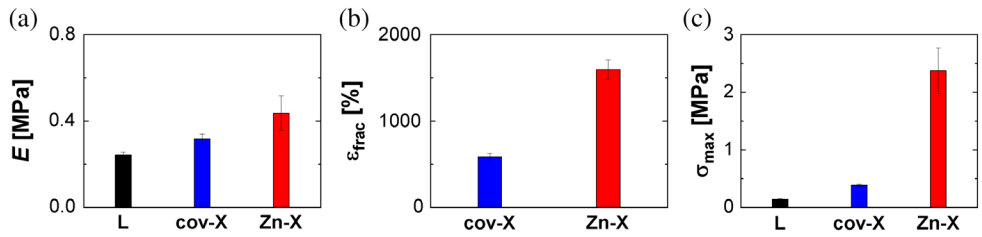

Figure 6. (a) Elastic modulus in the linear, low-strain regime, (b) strain at fracture, and (c) peak stress for L, cov-X, and Zn-X. [Color figure can be viewed at wileyonlinelibrary.com]

explanation for the decrease of f_m for DA-L and DA-Zn-X-0.5 is provided. In general, the acceleration of interdiffusion by hydroplasticization for DA-L and DA-Zn-X-0.5 is rather weakly pronounced. Although f_m does increase with increasing rH up to 75%, the changes do not seem to be significant (Figure 7). Again, all films dried at 92% rH were turbid. The turbidity is caused by light scattering. Light is scattered by water kept in the film by the hydrophilic, ionic surfactants which have been used to stabilize the particles.[56] In the herein studied dispersions, SDS, an anionic surfactant, was used. In general, surfactants redistribute in the final film during the film formation process. If the surfactant is insoluble in the polymer phase, as it is the case for SDS in poly(*n*-butyl acrylate), it can accumulate at the film–air and/or the film–substrate interface, assemble to form hydrophilic pockets in the film or remain at the particle boundaries.[57] The rearrangement scenario is not limited to one particular case, though. [57] Here, it is assumed that a fraction of SDS molecules is still located at the boundaries between deformed particles. Results of film formation studies based on different techniques have indicated that particles of low-T_g polymers can deform before drying has completed because of their softness.[3,6,58–60] Since the films dried at 92% are turbid, it is expected that they still contain a small amount of water. Remaining water in the film can be located between the SDS layers between neighboring particles. Experimentally, this has been observed by solid state nuclear magnetic resonance studies on dispersions which were stabilized by SDS and dried up to 95% solids content.[61] Previous studies have shown that hydrophilic layers by surfactants at the particle boundaries can retard the interdiffusion of the hydrophobic polymers.[62] In case of DA-L and DA-Zn-X-0.5 dried at 92% rH, the retardation of interdiffusion due to a barrier effect caused by the surfactants at the particle boundaries appears to be stronger than the acceleration of interdiffusion by hydroplasticization, which is assumed to ultimately slow down interdiffusion.

Next, the further increase of f_m when increasing rH from 75 to 92% observed in DA-Zn-X-1 is discussed. Despite an assumed barrier effect by surfactant layers between the particles, interdiffusion is faster at 92% rH compared with 75% rH. Note that at 92% rH, interdiffusion in DA-Zn-X-1 is still slower than in DA-L and DA-Zn-X-0.5. A reason for the further acceleration of interdiffusion for DA-Zn-X-1 at 92% could be that water in the film weakens the ionic bond between carboxylate groups in the polymers and Zn^{2+} cations. This has been observed for metal organic frameworks exposed to high humidities.[63–65] If the ionic bonds are weakened DA-Zn-X-1, chains can interdiffuse faster. In case of DA-Zn-X-0.5, the number of cross-links is smaller (40% gel content) than in DA-Zn-X-1 (80% gel content), and thus weakening the bond strength of the cross-links does not significantly accelerate interdiffusion.

CONCLUSION

ZnDMA can be used as a co-monomer to synthesize aqueous dispersions of ionically cross-linked acrylics. FRET studies have shown that polymer interdiffusion during the film formation of these dispersions is still possible even at high degrees of cross-linking. Polymers are capable of fully intermixing, and thus, continuous films can be made. Tensile tests are consistent with interdiffusion studies. Because interdiffusion in films from dispersions of ionically cross-linked polymers is possible, final films have both a higher peak stress and strain at failure compared with final films from dispersions of covalently cross-linked polymers in which almost no interdiffusion has taken place. Increasing the humidity accelerates interdiffusion in films from dispersions of ionically cross-linked polymers. Regarding a potential application, the results of this paper can be used to design dispersions of ionically cross-linked acrylic PSAs. From such dispersions, ionically cross-linked films can be made without the release of VOCs.

ACKNOWLEDGMENTS

The authors thank Martina Heinz and Martin Schwedes (both from the Institute of Technical Chemistry, Clausthal University of Technology, Germany) for GPC and DSC measurements, respectively. Tensile tests were performed by Dr. Rui de Oliveira and Ute Grau (both from BASF SE, Ludwigshafen, Germany) and are gratefully acknowledged. The authors thank Dr. Bastiaan Staal and co-workers (BASF SE, Ludwigshafen, Germany) for dye-sensitive GPC measurements.

REFERENCES

1. Keddie, J. L. *Mat. Sci. Eng. R Rep.* **1997**, *21*, 101.
2. Wang, Y.; Zhao, C.-L.; Winnik, M. A. *J. Chem. Phys.* **1991**, *95*, 2143.
3. Keddie, J. L.; Meredith, P.; Jones, R. A. L.; Donald, A. M. *Macromolecules*. **1995**, *28*, 2673.
4. Kim, K. D.; Sperling, L. H.; Klein, A.; Hammouda, B. *Macromolecules*. **1994**, *27*, 6841.
5. Pinenq, P.; Winnik, M. A.; Ernst, B.; Juhué, D. *J. Coat. Technol.* **2000**, *72*, 45.
6. Wahdat, H.; Gerst, M.; Rückel, M.; Möbius, S.; Adams, J. *Macromolecules*. **2019**, *52*, 271.
7. Zosel, A.; Ley, G. *Macromolecules*. **1993**, *26*, 2222.
8. van der Kooij, H. M.; van de Kerkhof, G. T.; Sprakel, J. *Soft Matter*. **2016**, *12*, 2858.
9. Taylor, J. W.; Winnik, M. A. *JCT Res.* **2004**, *1*, 163.
10. Czech, Z. *Polym. Int.* **2003**, *52*, 347.
11. Czech, Z.; Wojciechowicz, M. *Eur. Polym. J.* **2006**, *42*, 2153.
12. Tobing, S. D.; Klein, A. *J. Appl. Polym. Sci.* **2001**, *79*, 2230.
13. Bose, R. K.; Hohlbein, N.; Garcia, S. J.; Schmidt, A. M.; van der Zwaag, S. *Phys. Chem. Chem. Phys.* **2015**, *17*, 1697.
14. Mueller, E.; Alsop, R. J.; Scotti, A.; Bleuel, M.; Rheinstädter, M. C.; Richtering, W.; Hoare, T. *Langmuir*. **2018**, *34*, 1601.
15. Klingender, R. C.; Oyama, M.; Saito, Y. *Rubber World*. **1990**, *202*, 26.
16. Kitazono, E.; Minematsu, H.; Kawaguchi, T.; Miyoshi, T. (Teijin Limited). U.S. Patent 6,797,280, 29 January 2001.
17. Gerst, M.; Möbius, S.; Wulff, D.; Gross, M. (BASF SE). WO Patent 2018/141489 A1, 9 August 2018.

18. Taylor, D. W.; Freitag, J. W.; Howard, D. K. (Denovus LLC). WO Patent 2004/050740 A1, 17 June 2004.
19. Burfield, D. R. *J. Nat. Rub. Res.* **1986**, *1*, 202.
20. Kalista, S. J.; Ward, T. C. *J. R. Soc. Interface*. **2007**, *4*, 405.
21. Varley, R. J.; van der Zwaag, S. *Acta Mater.* **2008**, *56*, 5737.
22. Grande, A. M.; Castelnovo, L.; Landro, L. D.; Giacomuzzo, C.; Francesconi, A.; Rahman, M. A. *J. Appl. Polym. Sci.* **2013**, *130*, 1949.
23. Hird, B.; Eisenberg, A. *J. Polym. Sci. Part B: Polym. Phys.* **1990**, *28*, 1665.
24. Miwa, Y.; Kurachi, J.; Kohbara, Y.; Kustumizu, S. *Commun. Chem.* **2018**, *1*, 1.
25. Cai, Y.; Lapitsky, Y. *Colloids Surf. B Biointerfaces*. **2014**, *115*, 100.
26. Kalista, S. J., Jr.; Pflug, J. R.; Varley, R. J. *Polym. Chem.* **2013**, *4*, 4910.
27. Das, A.; Sallat, A.; Böhme, F.; Suckow, M.; Basu, D.; Wießner, S.; Stöckelhuber, K. W.; Voit, B.; Heinrich, G. *ACS Appl. Mater. Interfaces*. **2015**, *17*, 20623.
28. Xu, C.; Cao, L.; Lin, B.; Liang, X.; Chen, Y. *ACS Appl. Mater. Interfaces*. **2016**, *8*, 17728.
29. Hahn, K.; Ley, G.; Schuller, H.; Oberthür, R. *Colloid Polym. Sci.* **1986**, *264*, 1092.
30. Casier, R.; Gauthier, M.; Duhamel, J. *Macromolecules*. **2017**, *50*, 1635.
31. Jones, G. A.; Bradshaw, D. S. *Front. Phys.* **2019**, *7*, 1.
32. Boczar, E. M.; Dionne, C. B.; Fu, Z.; Kirk, A. B.; Lesko, P. M.; Koller, A. D. *Macromolecules*. **1993**, *26*, 5772.
33. Wahdat, H.; Hirth, C.; Johannsmann, D.; Gerst, M.; Rückel, M.; Adams, J. *Macromolecules*. **2018**, *51*, 4718.
34. Tronc, F.; Chen, W.; Winnik, M. A.; Eckersley, S. T.; Rose, G. D.; Weishuhn, J. M.; Meunier, D. M. *J. Polym. Sci. Part A: Polym. Chem.* **2002**, *40*, 4098.
35. Feng, J.; Pham, H.; MacDonald, P.; Winnik, M. A.; Geurts, J.; Zirkzee, H.; van Es, S.; German, A. L. J. *Coat. Technol.* **1998**, *70*, 57.
36. Pham, H. H.; Winnik, M. A. *J. Polym. Sci. Part A: Polym. Chem.* **2000**, *38*, 855.
37. Pham, H. H.; Winnik, M. A. *Macromolecules*. **2006**, *39*, 1425.
38. Aradian, A.; Raphaël, E.; de Gennes, P.-G. *Macromolecules*. **2000**, *33*, 9444.
39. Aradian, A.; Raphaël, E.; de Gennes, P.-G. *Macromolecules*. **2002**, *35*, 4036.
40. Tsavalas, J. G.; Sundberg, D. C. *Langmuir*. **2010**, *26*, 6960.
41. Soleimani, M.; Haley, J. C.; Lau, W.; Winnik, M. A. *Macromolecules*. **2010**, *43*, 975.
42. Haley, J. C.; Liu, Y.; Winnik, M. A.; Lau, W. *JCT Research*. **2008**, *5*, 157.
43. Gauthier, C.; Guyot, A.; Perez, J.; Sindt, O. In Provder, T.; Winnik, M. A.; Urban, M. W., Eds.; ACS Symposium Series 648; American Chemical Society: Washington, DC, **1996**; Chapter 10, p. 176.
44. Wang, Y.; Li, C.; Zhai, W.; He, Y.-F.; Song, P.; Xiong, Y.; Wang, R.-M. *Indian J. Chem. Sect A*. **2016**, *55*, 1167.
45. Landfester, K. *Angew. Chem. Int. Ed.* **2009**, *48*, 4488.
46. Turshatov, A.; Adams, J. *Polymer*. **2007**, *48*, 7444.
47. Ding, T.; Daniels, E. S.; El-Aasser, M. S.; Klein, A. *J. Appl. Polym. Sci.* **2005**, *97*, 248.
48. Santos, A. M.; Guillot, J.; McKenna, T. F. *Chem. Eng. Sci.* **1998**, *53*, 2148.
49. Musyanovych, A.; Rossmanith, R.; Tontsch, C.; Landfester, K. *Langmuir*. **2007**, *23*, 5367.
50. Kolthoff, I. M.; Miller, I. K. *J. Am. Chem. Soc.* **1951**, *73*, 3055.
51. Wang, Z.; Paine, A. J.; Rudin, A. *J. Polym. Sci. Part A: Polym. Chem.* **1995**, *33*, 1957.
52. Turshatov, A.; Adams, J.; Johannsmann, D. *Macromolecules*. **2008**, *41*, 5365.
53. Crank, J. The Mathematics of Diffusion. Clarendon Press: Oxford, UK, **1975**; Vol. *2*, Chapter 3, p 35.
54. de Gennes, P.-G. *J. Chem. Phys.* **1971**, *55*, 572.
55. Winnik, M. A.; Liu, Y. S. *Macromol. Symp.* **1995**, *92*, 321.
56. Liu, Y.; Gajewicz, A. M.; Rodin, V.; Soer, W.-J.; Scheerder, J.; Satgurunathan, G.; McDonald, P. J.; Keddie, J. L. *J. Polym. Sci. Part B: Polym. Phys.* **2016**, *54*, 1658.
57. Kientz, E.; Holl, Y. *Colloids Surf. A, Physicochem. Eng. Asp.* **1993**, *78*, 255.
58. Mallégol, J.; Gorce, J.-P.; Dupont, O.; Jeynes, C.; McDonald, P. J. *Langmuir*. **2002**, *18*, 4478.
59. Kimber, J. A.; Gerst, M.; Kazarian, S. G. *Langmuir*. **2014**, *30*, 13588.
60. Crowley, T. L.; Sanderson, A. R.; Morrison, J. D.; Barry, M. D.; Morton-Jones, A. J.; Rennie, A. R. *Langmuir*. **1992**, *8*, 2110.
61. Rottstegge, J.; Traub, B.; Wilhelm, M.; Landfester, K.; Heldmann, C.; Spiess, H. W. *Macromol. Chem. Phys.* **2003**, *204*, 787.
62. Pohl, K.; Adams, J.; Johannsmann, D. *Langmuir*. **2013**, *29*, 11317.
63. Low, J. J.; Benin, A. I.; Jakubczak, P.; Abrahamian, J. F.; Faheem, S. A.; Willis, R. R. *J. Am. Chem. Soc.* **2009**, *131*, 15834.
64. Canivet, J.; Fateeva, A.; Guo, Y.; Coasne, B.; Farrusseng, D. *Chem. Sov. Rev.* **2014**, *43*, 5594.
65. Schoenecker, P. M.; Carson, C. G.; Jasua, H.; Flemming, C. J. J.; Walton, K. S. *Ind. Eng. Chem. Res.* **2012**, *51*, 6513.